Soft Matter

Assembly of P3HT/CdSe nanowire networks in an insulating polymer host

Journal:	*Soft Matter*
Manuscript ID	SM-ART-05-2018-001001.R1
Article Type:	Paper
Date Submitted by the Author:	04-Jun-2018
Complete List of Authors:	Heo, Kyuyoung; Korea Research Institute of Chemical Technology, Miesch, Caroline; University of Massachusetts, Polymer Science and Engineering Na, Jun-Hee; Chungnam National University, Electric, Electronic and Comm. Engineering Edu. Emrick, Todd; University of Massachusetts-Amherst, Polymer Science and Engineering Hayward, Ryan; University of Massaschusetts, Polymer Science and Engineering

Soft Matter

PAPER

Assembly of P3HT/CdSe nanowire networks in an insulating polymer host

Received 00th May 2018,
Accepted 00th May 2018

DOI: 10.1039/x0xx00000x

Rsc.li/soft-matter-journal

Kyuyoung Heo,[a,b] Caroline Miesch,[a] Jun-Hee Na,[a] Todd Emrick,[a] and Ryan C. Hayward*[a]

Nanoparticles may act as compatibilizing agents for blending of immiscible polymers, leading to changes in blend morphology through a variety of mechanisms including interfacial adsorption, aggregation, and nucleation of polymer crystals. Herein, we report an approach to define highly structured donor/acceptor networks based on poly(3-hexylthiophene) (P3HT) and CdSe quantum dots (QDs) by demixing from an insulating polystyrene (PS) matrix. The incorporation of QDs led to laterally phase-separated co-continuous structures with sub-micrometer dimensions, and promoted crystallization of P3HT, yielding highly interconnected P3HT/QD hybrid nanowires embedded in the polymer matrix. These nanohybrid materials formed by controlling phase separation, interfacial activity, and crystallization within ternary donor/acceptor/insulator blends, offer attractive morphologies for potential use in optoelectronics.

Introduction

The addition of nanoparticles to polymers can yield significant enhancements in mechanical, thermal, electrical, and optical properties.[1-4] Achieving the largest improvements in properties often requires precise control over the location, organization, and state of dispersion of the particulate fillers. In the case of multicomponent nanocomposites formed using block copolymers[4-6] and polymer blends,[7-12] the selective localization of nanoparticles can also direct the nanoscale structure of the polymer matrix. For example, nanoparticles can kinetically stabilize co-continuous morphologies in blends by forming a percolating network of particles within one phase of a polymer mixture,[7,8] or by adsorbing to the interface between phases.[9-11]

Precise control of nanoscale structure is required to take full advantage of the unique properties of each component in optoelectronic devices such as photovoltaics[12-14] and photodetectors[15,16] based on conjugated polymers and quantum-confined nanocrystals. To achieve optimal performance, the materials must phase separate into interpenetrating domains with dimensions on the order of the exciton diffusion length (~ 10 nm).[17] Obtaining this level of intimate association of nanoparticles with semiconducting polymer hosts has been approached from several directions. This includes the introduction of polymer chain-end functionalities that associate directly with particle surfaces[18-20] or that chemically couple to the organic ligand shell,[21] as well as solution processes to promote association between nanoparticles and conducting polymer nanowires through favorable polymer/particle interactions,[22,23] co-crystallization of polymers with particle-grafted polymer ligands,[24] or crystallization-driven assembly.[25,26] The exclusion of particles during formation of crystalline polymer lamellae[27] provides well-defined nanoscale phase separated morphologies in blends of conjugated polymers with nanoparticles.

Blends of semiconducting polymers with insulating polymers have received attention due to the possibilities offered for enhancing mechanical robustness while simultaneously encapsulating the conjugated polymer to protect against oxidative degradation,[28] tune the electrical properties,[29-31] or provide stretchable devices.[32] However, the introduction of an insulating medium requires that the extent of demixing be controlled, to prevent loss of connectivity between domains of the semiconducting polymer that may diminish the desired optoelectronic properties.[28,33,34] To control the morphology of such blends, it is necessary to account for numerous factors including interfacial energy between polymers, surface energy, substrate interactions, and solubility of each component, as well as the kinetics of solvent evaporation. To date, however, the introduction of inorganic nanoparticles to mixtures of semiconducting and insulating polymers has not been widely explored.

Here, we examine demixing of nanoparticles from an insulating polymer matrix as a means to define the morphology of hybrid nanocomposites of semiconducting nanoparticles and polymers. Specifically, we consider blends of poly(3-hexyl thiophene) (P3HT), CdSe quantum dots (QDs), and polystyrene (PS), wherein the phase separation of P3HT and PS, coupled with the interfacial activity of CdSe, gives rise to interconnected P3HT nanowires decorated by CdSe nanoparticles. By comparing two samples of P3HT having markedly different degrees of crystallinity, we show that the crystallization of P3HT during aging in solution, and upon spin

[a] Polymer Science and Engineering Department, University of Massachusetts, Amherst, Massachusetts 01003, United States. E-mail: hayward@umass.edu
[b] Reliability Assessment Center, Korea Research Institute of Chemical Technology, Daejeon 34114, Republic of Korea.
† Electronic Supplementary Information (ESI) available. See DOI: 10.1039/x0xx00000x

coating, is critically important in generating the desired structures.

Experimental

Regioregular P3HT (M_n = 22.1 kg mol^{-1}, Đ = 2.34) was obtained from Rieke Metals and fractionated by progressive Sohxlet extractions with solvents of increasing solubility for P3HT (ethyl acetate, hexane, dichloromethane, chloroform).[35] PS (M_n = 62.0 kg mol^{-1}, Đ = 1.04) was purchased from Polymer Source and used without further purification. Tri-*n*-octylphosphine oxide-functionalized CdSe (CdSe–TOPO) QDs were prepared following a literature procedure[36] and repeatedly precipitated with a 3/10 (v/v) mixture of chloroform/methanol to remove excess ligands. The CdSe–PS QDs were obtained by ligand exchange using CdSe–TOPO QDs and thiol-terminated PS (PS–SH) (M_n = 3.6 kg mol^{-1}, Đ = 1.3). The PS–SH was synthesized by atom transfer radical polymerization (ATRP) as described in the literature.[37] Typically, CdSe–TOPO QDs (181 mg) were refluxed with pyridine (2 mL) under inert atmosphere for 24 h, and then precipitated into hexanes. The pyridine-covered QDs were heated overnight to 60 °C in anhydrous toluene (5 mL) containing PS-SH (300 mg). The CdSe–PS QDs were purified by precipitation into hexanes, centrifuged and washed with a 3/10 (v/v) chloroform/hexanes mixture.

To prepare blend films, appropriate quantities of P3HT, PS, CdSe–TOPO, and CdSe–PS QDs were dissolved in chloroform to yield a total concentration of 10 mg mL^{-1} with the desired composition. Thin film blend samples were prepared by spin coating onto appropriate substrates, for TEM and AFM (Si wafer with a 300 nm-thick SiO_2), and GIWAXS (Si wafer with native oxide) characterization. All films were dried overnight in a vacuum oven at 60 °C. To prepare the TEM samples, films on silicon wafers with a thick oxide layer were floated onto 5 wt% aqueous hydrofluoric acid solution and retrieved with a copper grid. To image the P3HT/SiO_2 interface, the floated films on hydrofluoric acid solution were transferred to a water bath and were subsequently captured on a Si wafer with the originally buried interface oriented upwards.

The molecular weight of P3HT was measured by gel permeation chromatography (GPC) in THF with polystyrene as calibration standard and a refractive index detector (Waters R4010). Bright field transmission electron microscopy (TEM) images were obtained using a JEOL 2000 FX microscope with an accelerating voltage of 200 keV. Surfaces and interfaces of the blend films were examined with a tapping mode atomic force microscope (Digital Instruments, Dimension-3000 AFM). Grazing–incidence wide–angle X-ray scattering (GIWAXS) measurements were carried out at beam line 11-3 of the Stanford Synchrotron Radiation Lightsource (SSRL). The thin films were measured at a sample-to-detector distance of 0.5 m using an X-ray radiation source of λ = 0.9744 nm. UV-vis absorption spectra were obtained with a Shimadzu UV 3600 spectrometer.

Results and discussion

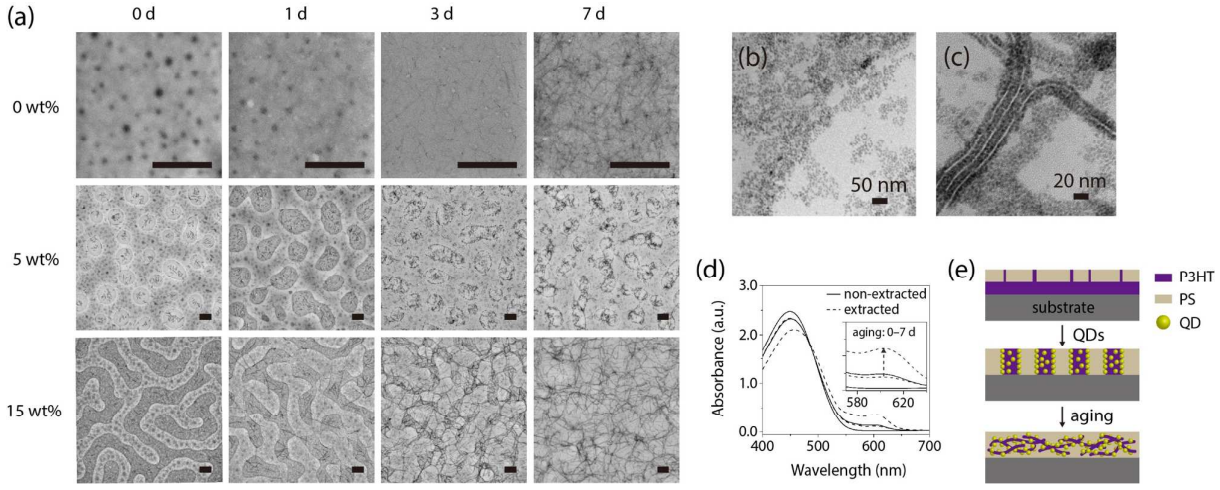

Fig. 1 (a) TEM images of P3HT/PS (50/50) blends as functions of solution aging time (0–7 d) and CdSe QD loading (0–15 wt%). Scale bars: 1 μm. (b, c) Magnification of images with (b) 0 d aging and (c) 7 d aging of P3HT/PS blends with 15 wt% CdSe QDs. The darker region in Figure (b) is the P3HT phase, and QDs concentrate at the P3HT/PS interface. (d) UV-vis absorption spectra of unextracted and extracted-P3HT solutions with respect to aging time. (e) Schematic illustration of QD-mediated phase separation between P3HT and PS, and hybrid nanowire formation.

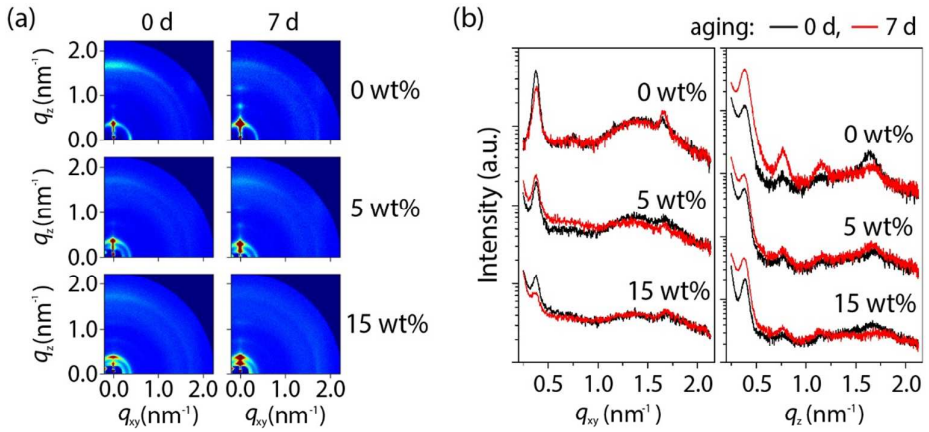

Fig. 2 GIWAXS data for P3HT/PS (50/50) blends as a function of solution aging time (0–7 d) and CdSe QD loading (0–15 wt%): (a) 2D GIWAXS images and (b) in-plane (q_{xy}) and out-of-plane (q_z) 1D GIWAXS profiles.

A summary of observed morphologies, as determined by transmission electron microscopy (TEM), is shown in Fig. 1a for blends spin-coated from chloroform as a function of two key parameters: 1) QD loading, and 2) the aging time of the solution prior to spin coating. In all cases, a Soxhlet-extracted sample of P3HT ($CHCl_3$ fraction: M_n = 22.6 kg mol^{-1}, Đ = 1.30, regioregularity = 94.9%) was used, and the ratio of P3HT:PS was maintained at 50:50 by weight. In the absence of QDs and without aging of the solution, a structure of circular domains with diameters of 130 ± 40 nm (corresponding to the P3HT-rich phase) was found. After immersing the film in cyclohexane (a solvent for PS and a non-solvent for P3HT) for 10 min, the film thickness was reduced from 92 to 35 nm. AFM images of these etched films (Fig. S1) clearly showed disk-like crystallites of P3HT that matched the sizes of the circular features seen by TEM, extending above a nearly uniform film of crystalline P3HT.[38] Based on these observations, we infer a structure as drawn in Fig. 1e, i.e., a bilayer structure with PS at the free surface, and protrusions of small P3HT domains into the PS layer. With aging of the solution prior to spin coating, increasing quantities of P3HT stripes (18 ± 4 nm in width) were seen, as shown along the top row of Fig. 1a. Although chloroform is a good solvent for P3HT, this structural evolution must reflect some degree of pre-crystallization in solution. Indeed, UV-vis measurements (Fig. 1d) confirmed that even a freshly prepared solution (stirred at 60 °C for 6 h) showed a weak absorption peak around 600 nm from semicrystalline P3HT aggregates,[39,40] which grew in intensity with aging. After aging the solution for 7 d prior to casting, the structure of spin-coated films evolved to highly interconnected P3HT nanowires in the insulating PS matrix, similar to the structures reported by Cho and co-workers for blends of P3HT and PS.[28]

Incorporating CdSe QDs (coated with the native tri-*n*-octyl phosphine oxide (TOPO) ligands) into the blends led to a dramatic morphological transition, as shown in the second and third rows of Fig. 1a. Without aging of the solution, 5 wt% of QDs yielded a laterally phase-separated structure consisting of isolated droplets of P3HT with sizes of 1.2 ± 0.3 μm in a matrix of PS. With 10 (Fig. S2) and 15 wt% (Fig. 1a) CdSe QDs, the structure evolved to a co-continuous morphology with characteristic domain widths of 1.0 ± 0.2 μm. The QDs were preferentially located in the P3HT phase, but were also enriched at the P3HT/PS interface (Fig. 1b). These observations suggest that the QDs act as interfacial modifiers that kinetically hinder demixing of PS and P3HT, stabilizing laterally separated morphologies, and even co-continuous structures at sufficiently high loadings. Given that the wetting behavior of the QDs is dictated by the TOPO ligands and therefore that their surface energy is likely to be similar to that of hydrocarbons ($\gamma_{hydrocarbon}$ ≈ 30–33 mN m^{-1}),[41] the interfacial adsorption of QDs is not surprising in light of the relatively high surface energy of PS (γ_{PS} = 40.7 mN m^{-1})[41] and low surface energy of P3HT (γ_{P3HT} = 21.0 ± 0.2 mN m^{-1}).[42] However, to confirm that interfacial activity of the QDs is responsible for the observed changes in structure, we performed experiments with PS-coated QDs,[8,43] which should locate preferentially in the PS phase. Indeed, the TEM image in Fig. S3 reveals that even with 15% loading of CdSe-PS QDs, the structure is very similar to that obtained without QDs, strongly supporting that interfacial activity of the TOPO-coated CdSe nanoparticles is key to the observed morphological changes. Since the presence of the insulating TOPO ligands is likely to have a deleterious effect on the electronic properties of the CdSe QDs,[44] we note that achieving similar interfacial localization with smaller ligands will be an important goal for future studies.

With longer aging times prior to casting the QD-loaded blend samples, an increasing number of crystalline nanowires could be seen within the P3HT domains. At a loading of 5 wt% QDs, however, the P3HT phase remained discontinuous and most of the nanowires were highly intertwined and localized within a single droplet of P3HT. This suggests that the preformed nanowires in solution are relatively short, and are

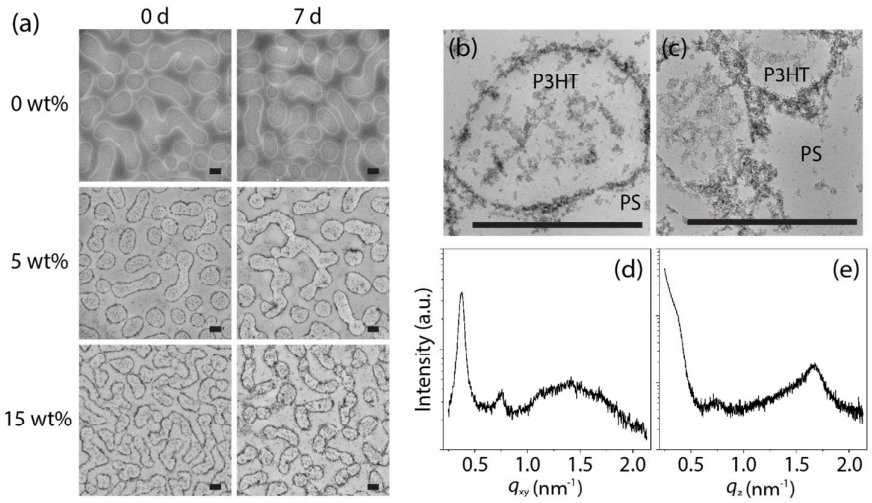

Fig. 3 (a) TEM images of unextracted-P3HT/PS (50/50) blends as functions of solution aging time (0–7 d) and CdSe QD loading (0–15 wt%). (b, c) Magnification of samples with 5 and 15 wt% QDs with 7 d aging from Figure (a) showing interfacial adsorption of CdSe. Scale bars: 1 µm. In-plane (d) and out-of-plane (e) 1D GIWAXS profiles of unextracted-P3HT/PS (50/50) blends for the sample with 15 wt% QDs without aging.

unable to grow substantially in length during solvent evaporation due to their confinement within the droplets. By contrast, at a loading of 15 wt% QDs, the co-continuous structure allowed for growth of a highly interconnected network of P3HT nanowires several micrometers in length. Furthermore, as shown in Fig. 1c, by 7 d of aging, the domains were reduced to 35 ± 11 nm in lateral dimension, which is only several times larger than the width of the individual P3HT nanowires. We propose that at sufficiently high loadings of QDs, the continuity of the P3HT domains is preserved during film formation, thus allowing the pre-existing nanowires in solution to grow substantially in length by further crystallization. Coupled with the localization of QDs to the PS/P3HT interface, this process results in a highly intermixed morphology of CdSe-decorated P3HT nanowires. While a loading of 15% of QDs is in the relevant range for photodetectors,[16] we note that future efforts to extend the strategy to greater QD contents would be beneficial for potential applications in photovoltaics, where peak efficiency in P3HT/CdSe devices usually requires higher loadings.[44,45]

Further insight into the structural evolution of these blend films was provided by grazing-incidence wide-angle X-ray scattering (GIWAXS), as summarized in Fig. 2. The P3HT/PS blend film without QDs showed a mixture of P3HT chain orientations (both face-on and edge-on) as indicated by the series of (h00) reflections along both the q_{xy} and q_z directions. The relatively strong (010) reflection along the q_z axis, corresponding to π–π interchain stacking, and the submicron-sized disk-like crystallites in the AFM phase image (Fig. S1b) are consistent with a substantial degree of face-on orientation, as quantified by comparing the intensity of the out-of-plane (q_z axis) to in-plane (q_{xy} axis) π-π stacking peaks from GIWAXS (Table S1).[46]

After 7 d of aging prior to spin coating, the blend films showed an increase in the overall degree of crystallinity and a shift to predominantly edge-on orientation, in keeping with the increased quantity of P3HT nanowires observed by TEM (Fig. 1a). We note that the orientation of P3HT crystals in thin films is a complex phenomenon influenced by solvent evaporation rate, solvent quality, polymer molecular weight/regioregularity, and substrate surface chemistry.[38,47,48] For P3HT spin coated from a volatile, good solvent such as $CHCl_3$, face-on stacking is generally favored due to a lack of time for the growth of edge-on oriented crystals. Here, pre-crystallization of P3HT during solution aging accelerates growth of P3HT crystals during spin casting, promoting the edge-on orientation. With the addition of CdSe QDs, the GIWAXS patterns showed both a weakening of the (010) reflection along the q_z axis and a strengthening of the (100) reflection along the q_z axis relative to the q_{xy} axis, indicating an increasing dominance of edge-on orientation. In

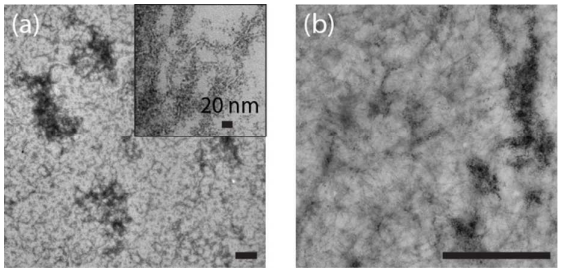

Fig. 4 (a) TEM image of an extracted-P3HT/CdSe (85/15) blend with 7 d of aging in the absence of PS. (b) TEM image of a blend of preformed P3HT nanowires, formed by addition of the poor solvent 1,4-dioxane, with PS and 15 wt% of CdSe QDs. Scale bars: 1 µm.

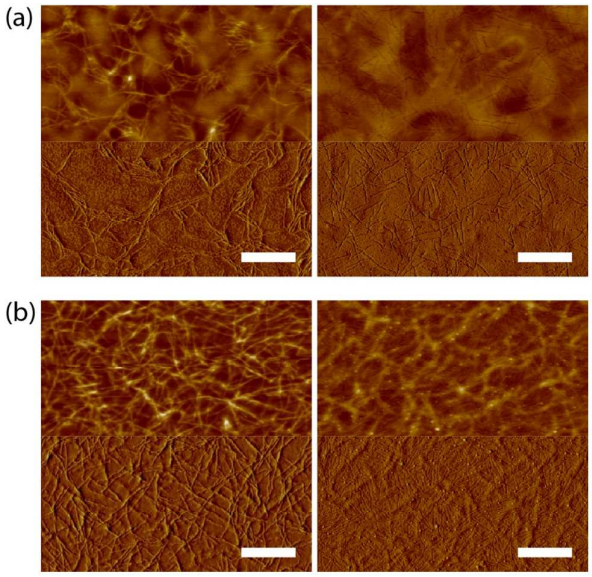

Fig. 5 AFM height (top) and phase (bottom) images of the free surface (left) and film/SiO_2 interface (right) of extracted-P3HT/PS/CdSe (42.5/42.5/15) thin films with (a) 3 d aging and (b) 7 d aging of solutions. Scale bars are 2 μm.

similar fashion to the blends lacking QDs, those containing P3HT also show an increase in edge-on orientation with solution aging.

To better understand the role of P3HT crystallization in driving the blend morphologies, we performed experiments using the as-synthesized polymer without Soxhlet extraction (M_n = 21.1 kg mol^{-1}, Đ = 2.34, regioregularity = 91.2%), which exhibits a much lower degree of crystallinity. As shown by TEM (Fig. 3a), blends without QDs exhibited laterally-phase separated structures consisting of droplets of P3HT in a PS matrix. GIWAXS (Figs. 3d and 3e) showed a weakly crystalline structure, with a preferred face-on stacking, as evidenced by the weak (h00) reflection along q_{xy} (in-plane) and stronger 010 reflection along q_z axis (out-of-plane), in agreement with a previous report.[48] It is noteworthy that these films exhibit a laterally separated structure, compared to the vertically phase-separated structure found without QDs and with no aging for extracted P3HT (Fig. 1a). Prior reports have established that P3HT and PS form vertically phase separated bilayer structures in the initial stages of spin coating due to the lower solubility of P3HT, followed by surface and interfacial instabilities that induce the transition to laterally phase separated structures.[49,50] Apparently, for the extracted P3HT system, solidification in the absence of QDs is much faster than the development of laterally-separated structures.

The addition of CdSe QDs to blends of PS with unextracted P3HT gave rise to interfacial adsorption of QDs (Fig. 3), and an evolution from droplets to a co-continuous structure, in similar fashion to the behavior of the unaged samples with extracted P3HT (Fig. 1a). For the unextracted material, however, aging for 7 d had little effect on the blend morphology; while some crystallization of material in solution could be seen by UV-vis (Fig. 1d), the amount of crystallinity after aging was comparable to that for unaged, extracted P3HT. These measurements confirm that both interfacial activity of CdSe QDs and crystallization of the P3HT component are essential to defining the highly interconnected hybrid nanowire networks seen in Fig. 1a.

We performed two additional experiments to gain further insight into the mechanism of structure formation. In the first case, we omitted PS from blends of 15 wt% CdSe QDs and extracted P3HT, with 7 d of aging. The resulting films (Fig. 4a) showed CdSe-decorated P3HT nanowires, but also much larger-scale aggregation of QDs compared to the network structures formed with PS. Similarly, blends of unextracted P3HT with CdSe QDs showed short P3HT nanowires and CdSe aggregates but no sign of interconnected network structures (Fig. S4). Thus, the PS matrix clearly plays an important role in defining the structures of the ternary blends, by enforcing co-assembly of P3HT nanowires and CdSe QDs within confined phase-separating domains. In the second case, we prepared preformed crystalline P3HT nanowires (see Fig. S5) by adding the poor solvent 1,4-dioxane to a solution of extracted P3HT in chloroform (1:5 by volume). Films cast from blends of these nanowires with PS and CdSe showed large-scale aggregation of QDs (Fig. 4b), rather than intimately associated hybrid structures, suggesting that the growth of the P3HT nanowire crystals during the process of blend demixing is also essential. Since one of the main factors affecting the performance of electronic devices is the structure at the active layer/gate dielectric interface, we investigated the interface between the buried film of extracted-P3HT/PS/CdSe (42.5/42.5/15) and SiO_2 layer. As shown in Fig. 5, the AFM imaging was very similar to that at the free surface, and consistent with the structures seen by TEM for a projection through the entire film thickness.

Conclusions

We have described an approach to define highly intermixed donor/acceptor network morphologies based on phase separation of P3HT and CdSe QDs from an insulating PS matrix. The adsorption of QDs to the P3HT/PS interface stabilizes co-continuous laterally phase-separated structures. Coupled with the crystallization of P3HT in solution and during film casting, this demixing defines interconnected nanoscale domains of P3HT nanowires decorated by CdSe nanoparticles. This combination of phase separation, interfacial segregation, and crystallization in multicomponent blends suggests a new strategy for creating materials with structures tailored for use in optoelectronics, photonics, and sensors.

Conflicts of interest

There are no conflicts to declare.

Acknowledgements

This work was supported by the U.S. Department of Energy, Office of Science, Basic Energy Sciences under Award #DE-SC0016208 (for self-assembly studies and morphological characterization), with additional support from the National Science Foundation through Grant CHE-1506839 (for quantum dot and polymer syntheses). The work also made use of facilities supported by the National Science Foundation MRSEC at UMass (DMR-0820506). We thank Yue Zhang for conducting the GIWAXS measurements. X-ray experiments were carried out at the Stanford Synchrotron Radiation Lightsource, a national user facility operated by Stanford University on behalf of the U.S. Department of Energy, Office of Basic Energy Sciences.

References

1 R. A. Vaia and J. F. Maguire, *Chem. Mater.*, 2007, **19**, 2736-2751.
2 J. Kao, K. Thorkelsson, P. Bai, B. J. Rancatore and T. Xu, *Chem. Soc. Rev.*, 2013, **42**, 2654-2678.
3 R. Mangal, S. Srivastava and L. A. Archer, *Nat. Commun.*, 2015, **6**, 7198.
4 M. R. Bockstaller, R. A. Mickiewicz and E. L. Thomas, *Adv. Mater.*, 2005, **17**, 1331-1349.
5 T. N. Hoheisel, K. Hur and U. B. Wiesner, *Prog. Polym. Sci.*, 2015, **40**, 3-32.
6 B. J. Kim, J. J. Chiu, G. R. Yi, D. J. Pine and E. J. Kramer, *Adv. Mater.*, 2005, **17**, 2618-2622.
7 G. W. Peng, F. Qiu, V. V. Ginzburg, D. Jasnow and A. C. Balazs, *Science*, 2000, **288**, 1802-1804.
8 L. Li, C. Miesch, P. K. Sudeep, A. C. Balazs, T. Emrick, T. P. Russell and R. C. Hayward, *Nano Lett.*, 2011, **11**, 1997-2003.
9 H. Chung, K. Ohno, T. Fukuda and R. J. Composto, *Nano Lett.*, 2005, **5**, 1878-1882.
10 E. M. Herzig, K. A. White, A. B. Schofield, W. C. K. Poon and P. S. Clegg, *Nat. Mater.*, 2007, **6**, 966-971.
11 S. Huang, L. Bai, M. Trifkovic, X. Cheng and C. W. Macosko, *Macromolecules*, 2016, **49**, 3911-3918.
12 W. U. Huynh, J. J. Dittmer and A. P. Alivisatos, *Science*, 2002, **295**, 2425-2427.
13 Y. Firdaus, R. Miranti, E. Fron, A. Khetubol, E. Vandenplas, D. Cheyns, H. Borchert, J. Parisi and M. V. d. Auweraer, *J. Appl. Phys.*, 2015, **118**, 055502.
14 C.-J. Chiang, Y.-H. Lee, Y.-P. Lee, G.-T. Lin, M.-H. Yang, L. Wang, C.-C. Hsieh and C.-A. Dai, *J. Mater. Chem. A*, 2016, **4**, 908-919.
15 G. Konstantatos, I. Howard, A. Fischer, S. Hoogland, J. Clifford, E. Klem, L. Levina and E. H. Sargent, *Nature*, 2006, **442**, 180-183.
16 J. Yoo, S. Jeong, S. Kim and J. H. Je, *Adv. Mater.*, 2015, **27**, 1712-1717.
17 P. E. Shaw, A. Ruseckas and I. D. W. Samuel, *Adv. Mater.*, 2008, **20**, 3516-3520.
18 J. S. Liu, T. Tanaka, K. Sivula, A. P. Alivisatos and J. M. J. Frechet, *J. Am. Chem. Soc.*, 2004, **126**, 6550-6551.
19 Q. Zhang, T. P. Russell and T. Emrick, *Chem. Mater.*, 2007, **19**, 3712-3716.
20 E. B. Pentzer, F. A. Bokel, R. C. Hayward and T. Emrick, *Adv. Mater.*, 2012, **24**, 2254-2258.
21 J. Xu, J. Wang, M. Mitchell, P. Mukherjee, M. Jeffries-El, J. W. Petrich and Z. Lin, *J. Am. Chem. Soc.*, 2007, **129**, 12828-12833.
22 J. J. Xu, J. C. Hu, X. F. Liu, X. H. Qiu and Z. X. Wei, *Macromol. Rapid Commun.*, 2009, **30**, 1419-1423.
23 S. Q. Ren, L. Y. Chang, S. K. Lim, J. Zhao, M. Smith, N. Zhao, V. Bulovic, M. Bawendi and S. Gradecak, *Nano Lett.*, 2011, **11**, 3998-4002.
24 F. A. Bokel, P. K. Sudeep, E. Pentzer, T. Emrick and R. C. Hayward, *Macromolecules*, 2011, **44**, 1768-1770.
25 Y.-J. Kim, C.-H. Cho, K. Paek, M. Jo, M.-k. Park, N.-E. Lee, Y.-j. Kim, B. J. Kim and E. Lee, *J. Am. Chem. Soc.*, 2014, **136**, 2767-2774.
26 S.-M. Jin, I. Kim, J. A. Lim, H. Ahn and E. Lee, *Adv. Funct. Mater.* 2016, **26**, 3226–3235.
27 M. Brinkmann, D. Aldakov and F. Chandezon, *Adv. Mater.*, 2007, **19**, 3819-3823.
28 L. Qiu, W. H. Lee, X. Wang, J. S. Kim, J. A. Lim, D. Kwak, S. Lee and K. Cho, *Adv. Mater.*, 2009, **21**, 1349-1353.
29 S. Goffri, C. Mueller, N. Stingelin-Stutzmann, D. W. Breiby, C. P. Radano, J. W. Andreasen, R. Thompson, R. A. J. Janssen, M. M. Nielsen, P. Smith and H. Sirringhaus, *Nat. Mater.*, 2006, **5**, 950-956.
30 H.-L. Cheng, J.-W. Lin, J. Ruan, C.-H. Lin, F.-C. Wu, W.-Y. Chou, C.-H. Chen, C.-K. Chang and H.-S. Sheu, *ACS Appl. Mater. Inter.*, 2015, **7**, 16486-16494.
31 G. Lu, N. Koch and D. Neher, *Appl. Phys. Lett.*, 2015, **107**, 063301.
32 E. Song, B. Kang, H. H. Choi, D. H. Sin, H. Lee, W. H. Lee and K. Cho, *Adv. Funct. Mater.*, 2016, **2**, 1500250.
33 J. Chen, Z. Chen, Y. Qu, G. Lu, F. Ye, S. Wang, H. Lv and X. Yang, *RSC Adv.*, 2015, **5**, 1777-1784.
34 M. Chang, D. Choi, G. Wang, N. Kleinhenz, N. Persson, B. Park and E. Reichmanis, *ACS Appl. Mater. Interfaces*, 2015, **7**, 14095-14103.
35 M. Trznadel, A. Pron, M. Zagorska, R. Chrzaszcz and J. Pielichowski, *Macromolecules*, 1998, **31**, 5051-5058.
36 Z. A. Peng and X. G. Peng, *J. Am. Chem. Soc.*, 2001, **123**, 183-184.
37 L. Garamszegi, C. Donzel, G. Carrot, T. Q. Nguyen and J. Hilborn, *React. Funct. Polym.*, 2003, **55**, 179-183.
38 D. H. Kim, Y. D. Park, Y. Jang, H. Yang, Y. H. Kim, J. I. Han, D. G. Moon, S. Park, T. Chang, C. Chang, M. Joo, C. Y. Ryu and K. Cho, *Adv. Funct. Mater.*, 2005, **15**, 77-82.
39 P. J. Brown, D. S. Thomas, A. Kohler, J. S. Wilson, J. S. Kim, C. M. Ramsdale, H. Sirringhaus and R. H. Friend, *Phy. Rev. B*, 2003, **67**, 064203.
40 S. Samitsu, T. Shimomura, S. Heike, T. Hashizume and K. Ito, *Macromolecules*, 2008, **41**, 8000-8010.

41 J. Brandrup, E. H. Immergut and E. A. Grulke, *Polymer Handbook*, JohnWiley & Sons, New York, 1999.
42 J. Jaczewska, I. Raptis, A. Budkowski, D. Goustouridis, J. Raczkowska, A. Sanopoulou, E. Pamula, A. Bernasik and J. Rysz, *Synth. Metals*, 2007, **157**, 726-732.
43 K. Sill and T. Emrick, *Chem. Mater.*, 2004, **16**, 1240-1243.
44 N. C. Greenham, X. Peng, and A. P. Alivisatos, *Phy. Rev B.*, 1996, **54**, 17628.
45 J. Seo, W. J. Kim, S. J. Kim, K.-S. Lee, A. N. Cartwright, and P. N. Prasad, *Appl. Phys. Lett.*, 2009, **94**, 133302.
46 J.-S. Kim, J.-H. Kim, W. Lee, H. Yu, H. J. kim, I. Song, M. Shin, J. H. Oh, U. Jeong, T.-S. Kim and B. J. Kim, *Macromolecules*, 2015, **48**, 4339.
47 D. M. DeLongchamp, B. M. Vogel, Y. Jung, M. C. Gurau, C. A. Richter, O. A. Kirillov, J. Obrzut, D. A. Fischer, S. Sambasivan, L. J. Richter and E. K. Lin, *Chem. Mater.*, 2005, **17**, 5610-5612.
48 H. H. Yang, S. W. LeFevre, C. Y. Ryu and Z. N. Bao, *Appl. Phys. Lett.*, 2007, **90**, 172116.
49 J. Jaczewska, A. Budkowski, A. Bernasik, I. Raptis, J. Raczkowska, D. Goustoruidis, J. Rysz and M. Sanopoulou, *J. Appl. Polym. Sci.*, 2007, **105**, 67-79.
50 J. Jaczewska, A. Budkowski, A. Bernasik, E. Moons and J. Rysz, *Macromolecules*, 2008, **41**, 4802-4810.

Table of contents

Hybrid nanowire networks of electron donors and acceptors were achieved by the combination of phase separation, interfacial segregation, and crystallization in multicomponent blends.